Hesterberg, L. K., & Lee, J. C. (1981) *Biochemistry 20*, 2974-2980.
Hesterberg, L. K., Lee, J. C., & Erickson, H. P. (1981) *J. Biol. Chem. 256*, 9724-9730.
Hill, D. E., & Hammes, G. G. (1975) *Biochemistry 14*, 203-213.
Hofer, H. W., & Pette, D. (1968) *Hoppe-Seyler's Z. Physiol. Chem. 349*, 1378-1392.
Howlett, G. J., & Schachman, H. K. (1977) *Biochemistry 16*, 5077-5083.
Lad, P. M., Hill, D. E., & Hammes, G. G. (1973) *Biochemistry 12*, 4303-4309.
Lee, J. C., Harrison, D., & Timasheff, S. N. (1975) *J. Biol. Chem. 250*, 9276-9282.
Leonard, K. R., & Walker, I. O. (1972) *Eur. J. Biochem. 26*, 442-448.
Ling, R. H., Marcus, F., & Lardy, H. A. (1965) *J. Biol. Chem. 240*, 1893-1899.
Mansour, T. (1972) *Curr. Top. Cell. Regul. 5*, 1-46.
Na, G. C., & Timasheff, S. N. (1980a) *Biochemistry 19*, 1347-1354.
Na, G. C., & Timasheff, S. N. (1980b) *Biochemistry 19*, 1355-1365.
Parmeggiani, A., Luft, J. H., Love, D. S., & Krebs, E. G. (1966) *J. Biol. Chem. 241*, 4625-4637.
Parr, G. R., & Hammes, G. G. (1975) *Biochemistry 14*, 1600-1605.
Parr, G. R., & Hammes, G. G. (1976) *Biochemistry 15*, 857-862.
Passonneau, J. V., & Lowry, O. H. (1963) *Biochem. Biophys. Res. Commun. 13*, 372-379.
Pavelich, M. J., & Hammes, G. G. (1973) *Biochemistry 12*, 1408-1414.
Pettigrew, D. W., & Frieden, C. (1979a) *J. Biol. Chem. 254*, 1887-1895.
Pettigrew, D. W., & Frieden, C. (1979b) *J. Biol. Chem. 254*, 1896-1961.
Reinhart, G. D., & Lardy, H. A. (1980) *Biochemistry 19*, 1484-1490.
Smith, G. D., & Schachman, H. K. (1973) *Biochemistry 12*, 3789-3801.
Uyeda, K. (1970) *J. Biol. Chem. 245*, 2268-2275.
Uyeda, K. (1979) *Adv. Enzymol. Relat. Areas Mol. Biol. 48*, 193-244.
Weisenberg, R. C., & Timasheff, S. N. (1970) *Biochemistry 9*, 4110-4116.
Wolfman, N. M., Thompson, W. R., & Hammes, G. G. (1978) *Biochemistry 17*, 1813-1817.
Wyman, J. (1964) *Adv. Protein Chem. 19*, 224-285.
Yount, R. G., Babcock, D., Ballantyne, W., & Ojala, D. (1971a) *Biochemistry 10*, 2484-2489.
Yount, R. G., Ojala, D., & Babcock, D. (1971b) *Biochemistry 10*, 2490-2496.

pH and Temperature Effects on the Molecular Conformation of the Porcine Pancreatic Secretory Trypsin Inhibitor As Detected by Hydrogen-1 Nuclear Magnetic Resonance†

Antonio De Marco,* Enea Menegatti, and Mario Guarneri

ABSTRACT: ^{1}H NMR spectra of the porcine pancreatic secretory trypsin inhibitor (PSTI) have been recorded vs. pH and temperature. Of the two tyrosines, one titrates with a pK of 11.25, while the resonances from the other are pH insensitive in the investigated range 4.8 ≤ pH ≤ 12. This is consistent with PSTI having one Tyr solvent exposed (Tyr-20) and the other buried (Tyr-31). The resonances from the lysyl ϵ-CH_2 protons titrate with a pK of 10.95. The titration is accompanied by a pronounced line broadening, which starts near pH 8.5. Between pH 11.5 and pH 12 the ϵ-CH_2 resonances recover their low pH line width. Titration curves for the lysines and Tyr-20 reflect single proton ionization equilibria, suggesting that these residues do not interact among themselves. On the basis of double resonance experiments, combined with analysis of chemical shifts, spin–spin couplings, and line widths, all methyl resonances are identified and followed as functions of pH and temperature. The γ-CH_3 doublet from the N-terminal Thr-1 is assigned by comparison between spectra of forms I and II of the inhibitor, the latter lacking the first four residues of form I. The β-CH_3 resonance from Ala-7 is also assigned. Proton resonance parameters of methyl groups are shown to afford useful NMR probes for the characterization of local nonbonded interactions, microenvironments, and mobilities.

In recent years there has been an increasing interest in serine proteases and their inhibitors. Among their numerous functions, serine proteases appear to have an important role in tumor promotion and hormone action, activities which are blocked by protease inhibitors (Troll et al., 1970; Katz et al., 1977). Proteases also participate in the survival "SOS" mechanism in mutagenesis in *Escherichia coli* (Witkin, 1976), an action that is blocked by specific inhibitors as well (Meyn et al., 1977).

Protease inhibitors define a class of small proteins. They have become extremely useful for the study of structural dynamics of globular polypeptides. The Kunitz trypsin inhibitor from bovine pancreas (BPTI)[1] is so far one of the best char-

† From the Istituto di Chimica delle Macromolecole del CNR, 20133 Milano, Italy (A.D.M.), and the Istituto di Chimica Farmaceutica dell'Università di Ferrara, 44100 Ferrara, Italy (E.M. and M.G.). *Received June 2, 1981.* This work was supported in part by grants from Lepetit S.p.A., Milano, and from the Progetto Finalizzato del CNR Chimica Fine e Secondaria.

[1] Abbreviations: NMR, nuclear magnetic resonance; ppm, parts per million; TSP, sodium 3-(trimethylsilyl)(2,2,3,3-$^2H_4$)propionate; UV, ultraviolet spectroscopy; PSTI, pancreatic secretory trypsin inhibitor; BPTI, basic pancreatic trypsin inhibitor; HPI, pancreatic trypsin inhibitor from *Helix pomatia*; CTI, pancreatic trypsin inhibitor from cow colostrum; FID, free induction decay.

0006-2960/82/0421-0222$01.25/0

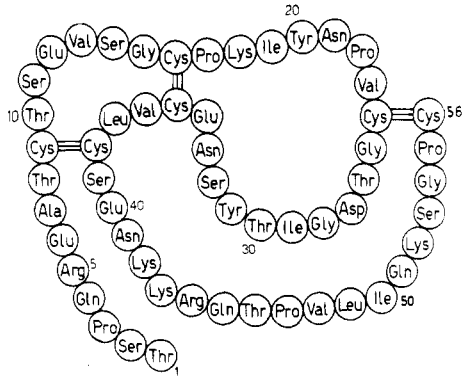

FIGURE 1: Primary structure of the porcine pancreatic secretory trypsin inhibitor (PSTI) (Tschesche & Wachter, 1970; Bartelt & Greene, 1971). Form I consists of residues 1–56; form II consists of residues 5–56.

acterized proteins, as its crystal structure has been extensively refined (Deisenhofer & Steigemann, 1975) and the solution conformation analyzed in detail by NMR techniques [see, e.g., Wagner & Wüthrich (1979) and references cited therein]. The bovine pancreas contains a second trypsin inhibitor of the Kazal type about which little is known besides the amino acid sequence (Tschesche & Wachter, 1970; Bartelt & Greene, 1971). While BPTI finds its homologues in snail (HPI) and cow colostrum (CTI), the secretory trypsin inhibitor of the Kazal type is closely related to the porcine, ovine, and human analogues (Greene & Bartelt, 1969; Tschesche & Wachter, 1970; Bartelt & Greene, 1971; Greene et al., 1976). This makes the study of Kazal inhibitors interesting in view of their potential clinical applications. In a previous ^{1}H NMR investigation (De Marco et al., 1979), we have reported preliminary conclusions on the solution conformation and dynamics of the pancreatic secretory trypsin inhibitor (PSTI) from porcine pancreas in its forms I and II, the latter lacking the first four residues of form I (Figure 1). In the present communication, we extend our previous analysis to the complete identification of methyl resonances in PSTI. Lysyl ϵ-CH_2 resonances are also identified and followed during pH titration, as well as the aromatic signals.

Experimental Procedures

The source of Kazal inhibitors was described elsewhere (De Marco et al., 1979). PSTI I and II solutions were both 2 mM in ^2H_2O. pH was adjusted by the addition of KO^{2}H or ^{2}HCl; no buffers were used. The pH meter readings are reported without correction for isotope effects. Labile protons were exchanged against deuterons by heating the samples in ^2H_2O solution at 75 °C, pH 4.8, for several hours. ^{1}H NMR spectra were recorded in the Fourier mode by using a Bruker HX-270 spectrometer. Between 2000 and 5000 scans were averaged for each spectrum with a repetition rate of 1.2 s and a flip angle of ca. 45°. Resonance positions were measured from internal dioxane, assumed to be at 3.766 ppm from TSP (De Marco, 1977). Resolution enhancement was achieved by multiplying the interferogram with polynomial functions (De Marco et al., 1979), which gives results comparable to those obtained by other techniques (Campbell et al., 1973; De Marco & Wüthrich, 1976). Computer simulation of spectra was performed with the NMRCAL program (Nicolet 1080 data package). The CH_3 resonances were individually calculated from their experimental intensities, chemical shifts, line widths, and coupling constants. The composite spectrum, resulting from superposition of Lorentzian line shapes was then Fourier transformed, subjected to the same digital filtering as the experimental FID, and again Fourier transformed to obtain a calculated spectrum accounting for the resolution enhancement distortion.

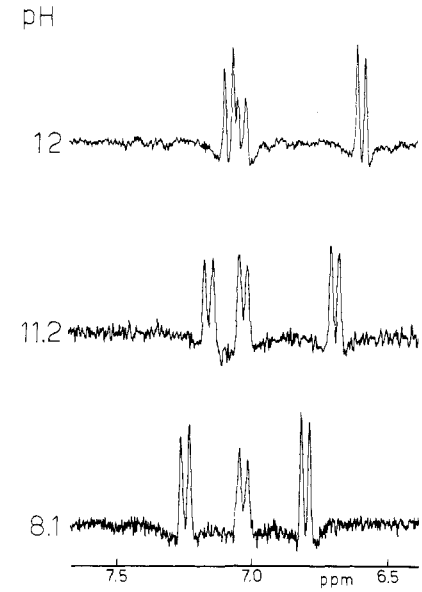

FIGURE 2: ^{1}H NMR spectra of PSTI I: aromatic resonances at pH 8.1, 11.2, and 12.0; T = 25 °C. Amide protons were previously exchanged against ^2H_2O.

Results

Aromatic Residues. Figure 2 shows the 6.5–7.5-ppm region of the PSTI I ^{1}H NMR spectrum at 270 MHz, at several pH values, after ^{1}H–^{2}H exchange of the labile protons. The inhibitor contains two tyrosines (Tyr-20 and Tyr-31) as the only aromatic residues (Figure 1). Therefore, the resonances in Figure 2 arise from two tyrosyl spin systems, each integrated by four protons. In a previous study (De Marco et al., 1979), we assigned the sharp, temperature-invariant AA′XX′ doublets at 6.8 and 7.25 ppm (Figure 2, pH 8.1) to the ϵ,ϵ' and δ,δ' ring protons of Tyr-20, respectively. The resonance pattern of Tyr-20 is characteristic of rapid ring motions through the entire pH and temperature range we have explored. The broader doublet at 7.03 ppm was then assigned to the ϵ,ϵ' proton resonances of Tyr-31, whose δ and δ' protons, below 40 °C, give resonances too broad to be observed after the application of resolution enhancement which deemphasizes the broader peaks. The ring resonances of Tyr-31 are temperature dependent and characteristic of a slow to rapid motion transition: between 40 and 50 °C the δ,δ' doublet sharpens and becomes clearly visible (De Marco et al., 1979).

The above interpretation is in full agreement with earlier conclusions based on UV pH titrations (Tschesche, 1967), which suggested that the two tyrosyl rings in the porcine inhibitor are not dynamically equivalent. From the UV experiments, it appears that one tyrosine is readily titrated and has an apparent pK of about 11, whereas the second residue starts to titrate only at very basic pH. This pK shift was ascribed to the fact that the second aromatic ring is buried in the interior of the protein. Figure 2 shows that, as a result of the phenol deprotonation, both Tyr-20 doublets move upfield with increasing pH while the doublet from Tyr-31 does not titrate below pH 12. Additional spectra taken at lower pH show that the Tyr-31 doublet remains at 7.031 ± 0.002 ppm in the range 4.8 ≤ pH ≤ 12. Tyr-20 has a pK of 11.25 for both pairs of δ,δ' and ϵ,ϵ' ring protons (see Table I). The titration data were fitted by assuming a single proton ionization equilibrium, since the slope of the pH vs. log $[(\delta_{HA} - \delta)/(\delta$

Table I: NMR Characteristics of Tyrosyl and Lysyl Proton Resonances in PSTI[a]

resonance	δ_{HA}	δ_{A^-}	$\delta_{HA} - \delta_{A^-}$	pK	s
δ,δ' Tyr-20	7.25	7.04	0.21	11.25	1.00
ϵ,ϵ' Tyr-20	6.81	6.55	0.26	11.25	0.99
ϵ,ϵ' Tyr-31[b]	7.03	7.03	0		
ϵ-CH_2 lysines[c]	3.02	2.63	0.39	10.95	1.00

[a] δ_{HA} and δ_{A^-} are the chemical shifts in ppm of the protonated and deprotonated forms, respectively. pK and s are the intercept and slope obtained from a linear regression fit of pH vs. log $[(\delta_{HA} - \delta)/(\delta - \delta_{A^-})]$ with a correlation coefficient $r^2 \geq 0.96$. [b] δ and δ' resonances are too broad to be measured with precision. [c] In the range $8.5 \leq$ pH ≤ 11.7, the resonances are degenerate and too broad to enable unequivocal assignment of signals to the four lysyl residues.

$- \delta_{A^-})]$ plot is 1.00 (see Table I). This suggests that Tyr-20 does not interact with other charged groups which titrate in the alkaline range and is consistent with the solvent exposure predicted for this aromatic side chain (De Marco et al., 1979).

Lysines. ^{1}H NMR resonances from lysyl ϵ-CH_2 groups in protein spectra usually appear as neat triplets at ca. 3 ppm, which shift to higher field positions as the pH is increased above ~9 (Brown et al., 1976). Their assignment is usually straightforward. Other methylene protons expected to resonate near 3 ppm would be the β-CH_2 from Asp, Asn, Cys, Phe, and Tyr (Bundi & Wüthrich, 1979). However, as such protons are closer to the backbone than those from ϵ-CH_2 Lys, their resonances are usually broader. In addition, while all such β resonances are decoupled by irradiating the corresponding α resonances near 4.7 ppm, the ϵ-CH_2 Lys multiplets are decoupled by irradiating the δ-CH_2 resonances at about 1.7 ppm.

PSTI contains four lysines, in positions 18, 42, 43, and 52. At pH 4.8 the ϵ-lysyl multiplet can be readily identified at ca. 3 ppm. By homonuclear irradiation of the δ-CH_2 signals at 1.7 ppm, the ϵ multiplet coalesces in two singlets of the same intensity but different line width (Figure 3). The sharp singlet impurity marked by a dot remains unaffected in the double resonance experiment and is pH invariant. The multiplet at 3 ppm has the expected intensity of eight protons, i.e., as determined by the ϵ-CH_2 resonances from four lysines. At pH 4.8 the four lysines in PSTI exhibit ϵ-CH_2 resonances equivalent in sets of two, both in chemical shift and line width. Moreover, for each methylene the geminal protons are degenerate, i.e., resonate exactly at the same position. Two ϵ-CH_2 signals appear at 3.04 ppm, exhibiting a line width of 5 Hz; the other two fall at 3.00 ppm, with a line width of ca. 8 Hz. The triplet splitting is 7.5 ± 0.2 Hz in both cases. A stick diagram indicates the two triplets in Figure 3. When the pH is increased, no effect is observed below ca. pH 8.5; above this pH, lysyl resonances move upfield as a result of deprotonation of the amino group, with concomitant line broadening, which reaches its maximum between 10 and 11 pH units and makes it impossible to separately follow the two sets of resonances. At pH 12 resonances have become sharp again and apparently split into the two triplets already observed at lower pH.

Due to broadening, it was possible to extract only average parameters, reported in Table I. Lysines titrate with a pK of 10.95 and a logarithmic plot slope of 1.00, which confirms the lack of interaction with Tyr-20.

Identification of Methyl Resonances. The amino acid sequence of PSTI I (Figure 1) contains sixteen residues with methyl groups: Ala-7; six Thr at positions 1, 8, 10, 26, 30, and 46; four Val at positions 13, 23, 36, and 48; two Leu at positions 37 and 49; three Ile at positions 19, 29, and 50. Ile-19 is of particular interest, since it is located at the active site (Bartelt & Greene, 1971). PSTI does not contain methionines. Except for the $C^{\delta}H_3$–$C^{\gamma}H_2$– group present in isoleucyl residues, the above-mentioned amino acids contain the CH_3–CH– fragment, so that in the ^{1}H NMR spectrum of PSTI I we expect to find 22 methyl doublets and 3 methyl triplets due to ^3J interaction with the vicinal protons. Figure 4 shows the $0 \leq \delta \leq 1.5$ ppm spectral region of PSTI I and II; sharp resonances are emphasized by digital filtering so that the spectrum results essentially from the methyl protons.

Homonuclear decoupling experiments enable us to derive a first classification of methyl groups. In random-coiled polypeptides α-CH Ala and β-CH Thr resonate at ca. 4.3 ppm. On the other hand, β-CH Val, β-CH Ile, γ-CH_2 Ile, and γ-CH Leu groups all appear between 1.2 and 2.1 ppm from TSP

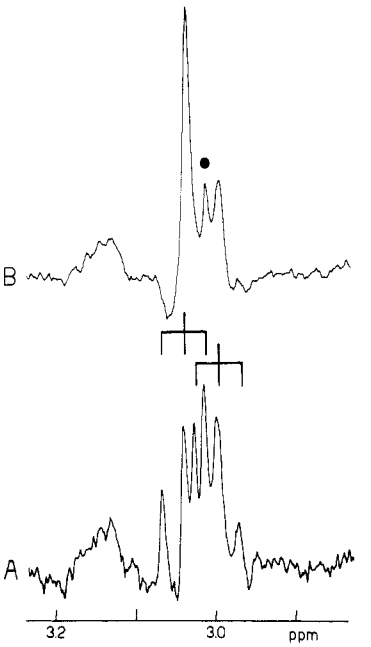

FIGURE 3: ^{1}H NMR spectra of PSTI: ϵ-CH_2 lysyl resonances, unperturbed (A) and under homonuclear irradiation of the coupled δ-CH_2 resonances at 1.7 ppm (B). T = 25 °C; pH 4.8. A singlet impurity is denoted by (●). As indicated by the stick diagram, the five signals in (A) result from partial overlap of two triplets, each accounting for the ϵ-CH_2 resonances from two lysines.

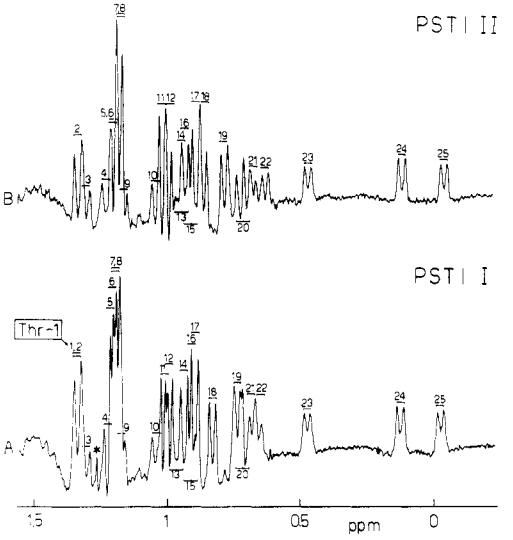

FIGURE 4: ^{1}H NMR spectra of PSTI I and II: methyl region, after resolution enhancement; pH ≈6.5; T = 25 °C. Methyl resonances are numbered from low to high field; (*) denotes an impurity.

Table II: Characteristics of Methyl Resonances in the ^{1}H NMR Spectrum of PSTI I at 25 °C, pH 4.8[a]

CH_3 no.	amino acid type	δ (ppm)	decoupling frequency (ppm)	^3J[b] (Hz)	LW[b] (Hz)
1	Thr-1	1.344 (1.31)[c]	4.1 (4.22)[c]	6.4 (6.3–6.6)	6.0
2	Ala-7	1.337 (1.39)	4.4 (4.35)	7.3 (7.0–7.3)	6.0
3, 7	Val	1.307, 1.194 (0.97, 0.94)	2.2 (2.13)	7.0 (6.9–7.0)	8.0, 4.5
4	Thr	1.228			6.0
5	Thr	1.208			
6	Thr	1.196 (1.23)	4.1–4.4 (4.22)[d]	6.0–6.4 (6.3–6.6)[d]	4.5[d]
8	Thr	1.186			
9	Thr	1.176			6.0
10	γ-Ile	1.052 (0.94)	1.9 (1.89)	6.3 (6.9–7.0)	8.0
11, 12	Val	1.017, 1.002 (0.97, 0.94)	2.2 (2.13)	7.0 (6.9–7.0)	5.0, 5.0
13	δ-Ile	0.973 (0.89)	1.1 (1.48, 1.19)	7.2 (7.0–7.3)	9.0
14	γ-Ile	0.944 (0.94)	1.4 (1.89)	6.8 (6.9–7.0)	5.0
15	δ-Ile	0.916 (0.89)	1.5 (1.48, 1.19)	7.2 (7.0–7.3)	9.0
16	γ-Ile	0.912 (0.94)	1.7 (1.89)	6.8 (6.9–7.0)	9.0
17, 18	Leu	0.903, 0.838 (0.94, 0.90)	1.7 (1.65)	6.3 (6.3–6.5)	5.0, 6.0
19, 22	Leu	0.747, 0.665 (0.94, 0.90)	1.7 (1.65)	6.3 (6.3–6.5)	6.0, 8.0
20	δ-Ile	0.724 (0.89)	1.2 (1.48, 1.19)	7.2 (7.0–7.3)	6.0
21, 24	Val	0.688, 0.134, (0.97, 0.94)	2.1 (2.13)	7.0 (6.9–7.0)	8.5, 8.5
23, 25	Val	0.483, −0.015 (0.97, 0.94)	1.1 (2.13)	6.8 (6.9–7.0)	9.0, 9.0

[a] Resonance numbers are as in Figure 4. Parameter values result from the calculated spectrum shown in Figure 5A′; δ, ^3J, and LW denote chemical shifts, vicinal coupling constants, and the line width of methyl resonances, respectively. The methyl-decoupling frequencies are also indicated. Methyl and methyl-coupled resonance frequencies (Bundi & Wüthrich, 1979; Campbell et al., 1975a) are reported in parentheses. [b] ±0.3 Hz (digital resolution). [c] Chemical shift values for an N-terminal threonine at acidic pH are from Ptak et al. (1978). [d] Due to overlap among threonyl resonances, only average parameters are reported.

(Bundi & Wüthrich, 1979). In globular proteins, ring currents or any other conformational effects can alter the above values. In PSTI only two noninteracting aromatic rings are present (De Marco et al., 1979), and it appears improbable that structural strain would cause the $\Delta\delta \geq 2.2$ ppm required to displace a CH_3-coupled signal from one group of resonances to the other. Consequently, by irradiating between 4.0 and 4.5 ppm, we expect to perturb β-Ala or γ-Thr methyl resonances, while all other methyls should be decoupled by applying the radiofrequency between ca. 1 and 2.5 ppm. However, even with large conformational shifts, the separation between coupled resonances does not usually deviate by more than about 0.5 ppm from that observed in the random-coil situation (Campbell et al., 1975a). As it can be estimated from Table II, such chemical shift separation is expected to be about 3 ppm for alanines and threonines and ≤1.2 ppm for the other residues. Besides the triplet pattern, which makes unequivocal the identification of δ-Ile CH_3 resonances, the coupling constants between methyls and their vicinal protons have already been recognized as an aid in assigning CH_3 resonances to specific types of amino acids (Campbell et al., 1975a,b). Table II shows that $^3J(CH–CH_3)$ is ≳7 Hz for β-Ala, γ-Val, γ-Ile, and δ-Ile, and ≤6.6 Hz for γ-Thr and δ-Leu methyls, the difference arising from the electronegativity of the substituents at the CH group (Bothner-By, 1970). Considering that irradiation of β-CH Val and γ-CH Leu decouples two methyls at once, while all other CH groups interact with one methyl only, the simple criteria so far presented in the absence of accidental degeneracies are per se sufficient to allow for a classification of CH_3 resonances as arising from various types of amino acids.

Alanines and Threonines. Systematic irradiation of the PSTI I spectrum between 4.0 and 4.5 ppm decouples the quasi-coincident doublets at 1.34 ppm, marked 1 and 2 in Figure 4A, and perturbs the intense degenerate multiplet at ca. 1.2 ppm. As checked by simulation (Figure 5), such multiplet has the intensity of six methyls. By irradiating at 2.25 ppm, we decouple doublet 3, together with doublet 7. Since it is reasonable to assume that these two doublets are of the Val or Leu type, between 1.2 and 1.4 ppm, we are left with seven Ala plus Thr doublets, which is in agreement with the amino acid composition. Of the six threonines in PSTI I, one is N terminal. At pH 12 the methyl 1 signal has moved toward the large multiplet at 1.2 ppm (Figure 5). This makes it possible to measure a 7.3-Hz doublet splitting for the CH_3 resonance labeled 2, while all other doublets between 1.2 and 1.4 ppm exhibit splittings of 6.4 ± 0.4 Hz. In PSTI II, methyl 1 is missing (Figure 4): the spectral region between 1.2 and 1.4 ppm accounts for eight methyl groups instead of the nine found for the inhibitor I. From these results we conclude that (1) CH_3 1 can be assigned to the N-terminal Thr-1 in PSTI I, since it is absent in PSTI II and titrates in the pH range close to the pK_a of NH_3^+ group, (2) CH_3 marked 2 is assigned to Ala-7 because of the relatively large coupling constant $^3J(CH_3–CH)$, and (3) the remaining five threonyl methyls of PSTI I resonate between 1.18 and 1.23 ppm, i.e., at the random-coil position of such groups in polypeptides (Table II).

Decoupling experiments in PSTI II lead to essentially identical results, except for the already noted absence of the CH_3 resonance from Thr-1 (Figure 4B).

Valines, Leucines, and Isoleucines. The isoleucyl triplet marked 20 in Figure 4A was readily identified by irradiation at 1.2 ppm. Application of the decoupling frequency at 1.5 and 1.1 ppm caused the appearance of two singlet lines at 0.92 and 0.97 ppm, which are not centered on doublets in the undecoupled spectrum. These positions were hence assigned to the δ-CH_3 triplets from the two remaining Ile residues, relatively broad and masked by other signals in the unperturbed spectrum. Irradiating between 1.0 and 2.3 ppm caused perturbation of the remaining CH_3 lines, which could be interpreted as representing 13 doublets. This completes the expected total of 25 methyls. The latter 13 doublets arise from γ-Val, δ-Leu, and γ-Ile resonances.

The NMR characteristics and the identification of methyl resonances in PSTI I are reported in Table II, together with the corresponding chemical shifts and coupling constants predicted for random-coil polypeptides (Bundi & Wüthrich, 1979; Campbell et al., 1975a) and for the particular case of a threonyl residue in the N-terminal position (Ptak et al., 1978). The pairing 17–18 and 19–22 for the leucyl residues is tentative and based on chemical shift and line width considerations that are discussed below. It can be noticed that doublet 10, assigned to a γ-Ile group on the basis of its decoupling frequency exhibits too small a ^3J splitting, ca. 6.3 Hz

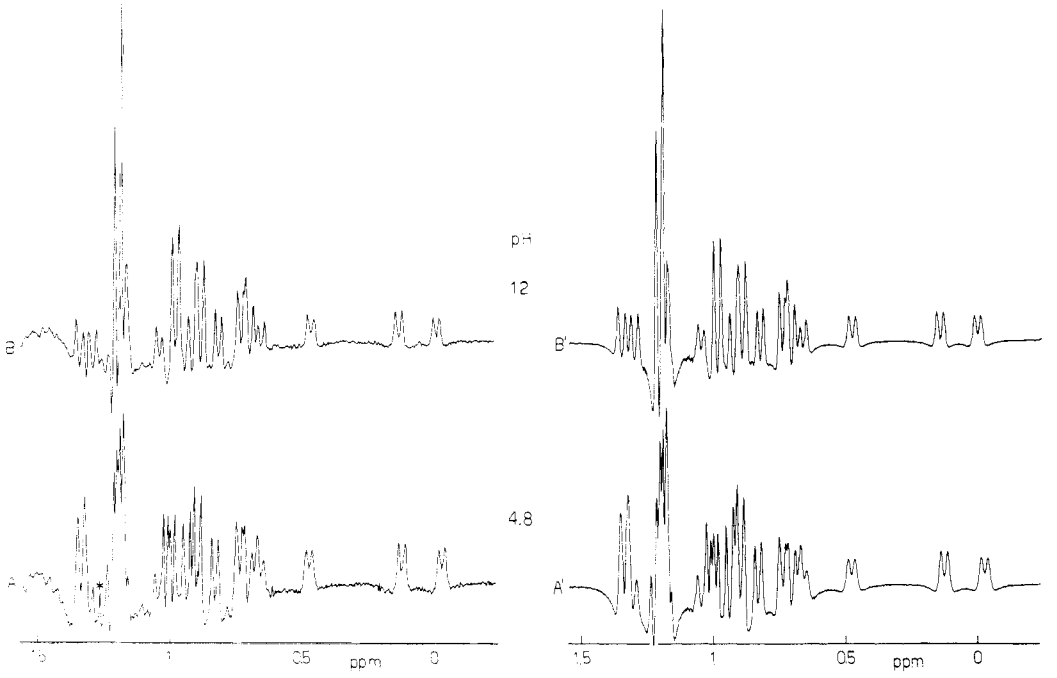

FIGURE 5: ^{1}H NMR spectra of PSTI I: methyl region, at 25 °C, after resolution enhancement. (A) pH 4.8; (B) pH 12.0; (A′) and (B′) are computer simulations of (A) and (B), respectively.

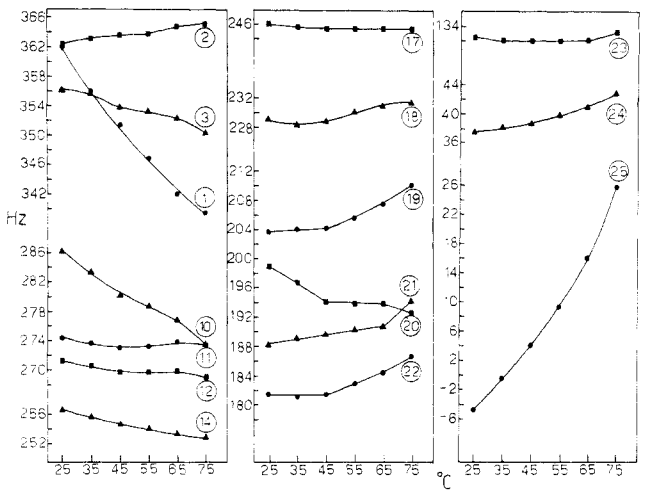

FIGURE 6: Temperature dependence of selected methyl resonances, in the ^{1}H NMR spectrum of PSTI I. Labeling is the same as in Figure 4. Solid lines result from arbitrary interpolations between points.

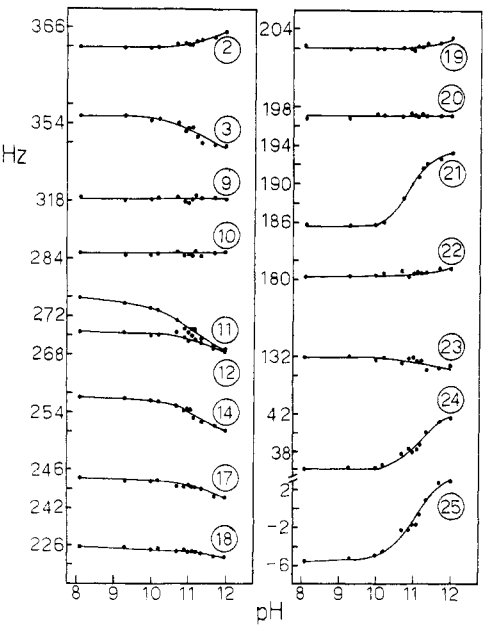

FIGURE 7: pH dependence of selected methyl resonances in the ^{1}H NMR spectrum of PSTI I. Labeling is the same as in Figure 4. Solid lines result from arbitrary interpolations between points.

vs. the expected ca. 7 Hz for such a group. However, the signal is somewhat broad, and a short T_1 of the coupled CH could induce an apparent reduction of the splitting on the methyl group (Navon & Polak, 1974). The complete identification of methyl resonances was achieved also for PSTI II, whose spectrum is shown in Figure 4B. The only resonances which are appreciably shifted in the absence of the N-terminal tetrapeptide are all of leucyl type, i.e., doublets 18 and 19 which move to lower fields by 0.04–0.05 ppm and 22 which moves upfield by 0.023 ppm. The other methyl resonances of PSTI II are in the same position as in PSTI I, ±0.01 ppm.

Temperature Dependence of Methyl Resonances in PSTI. Figure 6 shows the temperature dependence of 16 methyl resonances in PSTI I, labeled as in Figure 4. On going from 25 to 75 °C, it is noticed that (1) 2, 11, 12, 14, 17, 18, and 23 show negligible temperature dependence ($\Delta\delta \leq 4$ Hz), (2) 3, 10, 19, 20, 21, 22, and 24 show a temperature dependence varying between 5 and 13 Hz, and (3) 1 and 25 exhibit the strongest temperature effects (between 25 and 75 °C their positions change by 23 and 31 Hz, respectively).

Methyls attached to the same CH group do not show a uniform trend. Valine methyls 11–12 exhibit similar temperature dependences and the same applies to the couple 21–24; in contrast, methyls 23–25 manifest quite different temperature effects, indicative of distinct microenvironments for the two geminal groups. Leu resonances 17–18 exhibit little temperature dependence, while 19–22 move in parallel, being temperature insensitive up to ca. 50 °C, and shift continuously to lower fields with further temperature increase. This leads to tentative pairing of 17–18 and 19–22. In PSTI II the temperature dependence of CH_3 signals between 25 and 55 °C follows that of PSTI I within 2 Hz. The absence of a strongly temperature shifted methyl resonance near 1.3 ppm confirms the assignment of the Thr-1 doublet in PSTI I.

pH Dependence of Methyl Resonances in PSTI. Figure 7 shows the pH dependence of 16 methyl resonances in PSTI I. As observed when the temperature is raised, pH does not appreciably affect the chemical shift of a number of methyl resonances (9, 10, 18, 19, 20, 22, and 23); other signals are significantly shifted (2, 3, 11, 12, 14, and 17), while only three doublets (21, 24, and 25) exhibit the typical pH dependence of chemical shifts. Also consistent with the temperature perturbation effects (Figure 6), increasing pH shifts 17–18 and 19–22 in a uniform way. Again, 11–12 and 21–24 behave similarly while 23–25 differ.

Figure 5 shows the methyl region of PSTI I at pH 4.8 and 12. It is observed that the spectrum at pH 12 is characteristic of a native protein and very similar to the spectrum at pH 4.8: lines are equally sharp and no spurious signals from denatured species show up.

The observed chemical shifts, coupling constants, and line widths were used to calculate the spectrum (see Experimental Procedures) and slightly adjusted, until a satisfactory fitting was obtained. The result is shown in Figure 5A′,B′. The NMR characteristics of PSTI I at pH 4.8 are reported in Table II. At pH 12 the multiplet near 1.2 ppm contains 7 methyls, i.e., one more than at pH 4.8, while only two doublets appear between 1.3 and 1.5 ppm (three doublets at pH 4.8). This was rationalized above as due to a shift of the Thr-1 γ-CH_3 signal, following the deprotonation of the NH_3^+ group. The titration of the Thr-1 methyl could not be completed because of extensive degeneracy between 1.15 and 1.35 ppm.

Discussion

A wide range of motional situations has been observed for the aromatic side chains in various proteins. For tyrosines the immobilization results in a strong pK shift, caused by a decreased solvent accessibility. Hence, the pH invariance of Tyr-31 resonances in PSTI reflects a common feature observed in globular proteins. Among recent examples, in the homologous neurotoxin I and cardiotoxin V^{II}4 from *Naja mossambica mossambica*, Tyr-25, located in a densely packed hydrophobic cluster, has a pK value $\gtrsim$ 12 (Lauterwein et al., 1978). In the phosphocarrier protein HPr, the ring protons from the buried Tyr-6 are not titrable before denaturation of the protein (Schmidth-Aderjan et al., 1979). From these above examples, it appears that the dynamics of aromatic side chains is not appreciably changed during alkaline titration, unless concomitant denaturation occurs. It has been recognized that the packing of hydrophobic domains which enclose aromatic side chains is remarkably resistant to conventional denaturing conditions, pH in particular (Cramer et al., 1980). Hydrophobic pockets are preserved in the unfolding reactions which allow for fast amide proton exchange. The mobility of the aromatic rings would thus appear to correlate with the internal flexibility of the local hydrophobic cores (Wüthrich & Wagner, 1978).

For all lysyl residues in PSTI, the chemical shift equivalence between ϵ and ϵ' protons in geminal pairs, together with the 7.5-Hz triplet splitting observed for the vicinal coupling constant $^3J(^1H^{\delta}-^1H^{\epsilon})$, indicates an equal distribution of conformers about the $C^{\delta}-C^{\epsilon}$ bond and extensive flexibility for the side chains. On the other hand, the line width pattern and the relatively high pK of 10.95 favor a partial solvent accessibility for the lysyl residues; two lysines seem to be in a different environment than the other two.

The broadening of lysyl resonances could not be quantitatively evaluated. A rough estimate gives a maximum line width increase of 20–30 Hz. This strong titration broadening was not observed in BPTI (Brown et al., 1976) and may represent a peculiar dynamics of lysyl residues in PSTI.

Several hypotheses can be formulated to account for the observation. (1) The spectrum is an average of spectra arising from various protein conformers. In the pH range of the Lys titration, a population of states with unusual chemical shifts could result from various types of interactions between lysines and carboxylated side chains, such as H bonds or salt bridges. Since the averaging in the spectrum goes over a wide chemical shift range, broader resonances could result. (2) Conformational constraints on the Lys side chains could slow down the protonation–deprotonation reaction by raising the activation energy for the process. This would explain the broadening on the titrating group itself. It is well-known that the protonation–deprotonation mechanism of a charged group is strongly affected by its environment. As an example, a whole range of titration behaviors was argued for histidine residues according to the microdynamics of the imidazole rings (Markley, 1975). (3) Line broadening could also result from simple aggregation, i.e., pH-dependent protein association. However, if this were the case, one would expect a more uniform effect, while the line broadening observed between pH 10 and pH 11 is much stronger for the ϵ-CH_2 Lys resonances than for any other signal.

Aromatic–methyl interactions arising from the three-dimensional folding of the proteins have long been recognized (Sternlicht & Wilson, 1967). Recent studies on the basic pancreatic trypsin inhibitor indicate that ring current effects are the dominant contribution to the shifts of the peripheral aliphatic sidechain proton resonances from their random-coil positions (Perkins & Wüthrich, 1979). Table II reports the chemical shifts of methyl groups in PSTI I. While Ala-7 and all Thr methyls resonate near the random-coil position, the other residues, especially Val, spread over an ca. 1.3-ppm chemical shift range. Such a distribution of chemical shifts can be ascribed to ring current effects from the buried, pH-insensitive Tyr-31, rather than Tyr-20, free and solvent exposed, near the active site of the inhibitor (Bartelt & Greene, 1971).

Methyls near ionizable groups may exhibit a pH dependence indicative of nonbonded intramolecular contacts. Figure 7 shows that among the ring current shifted methyl resonances, only those labeled 21, 24, and 25 exhibit a definite titration shift between pH 10 and pH 12. This is in apparent contradiction with the hypothesis of the vicinity of such groups to the nontitrable Tyr-31. Within a pK range of $\pm$0.04, a chemical shift vs. pH plot for resonances 21, 24, and 25 yields pK = 10.95 for the three methyls (correlation coefficient $r^2 \gtrsim 0.98$). As reported above, the four lysines in PSTI titrate with a pK of ca. 10.95, against the pK = 11.25 measured for the deprotonation of Tyr-20. The difference is significant: the pK value found for the titration of the methyl groups suggest that one or more lysines are part of the hydrophobic pocket surrounding the aromatic residue. In this model, the lysines are still sufficiently accessible to the solvent to allow for deprotonation of their NH_3^+ groups. The different pH dependence of methyls 23 and 25 from the same valine (Figure 7) indicates a different microenvironment for the geminal groups and hence a restricted mobility about the $C^{\alpha}-C^{\beta}$ bond. In contrast geminal methyls 11 and 12 exhibit a similar pH dependence, and the same applies to the pairs 17–18, 19–22, and 21–24, which could result from free rotation of the isopropyl groups. This is mirrored in the effect of temperature on the chemical shift of the same CH_3 groups, as shown in Figure 6. Methyl 25 has the strongest temperature dependence of all methyls, shifting by ca. 0.12 ppm downfield between 25

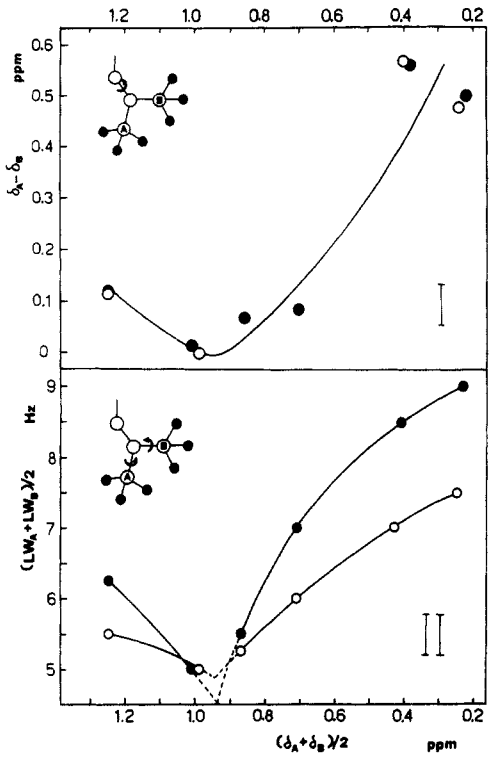

FIGURE 8: (I) Chemical shift difference ($\delta_A - \delta_B$) between A and B geminal methyl signals of the six Val or Leu (Table II) plotted against the average chemical shift of each pair, $(\delta_A + \delta_B)/2$, at pH 4.8 (●) and 12.0 (○). In two cases, near $(\delta_A + \delta_B)/2 \approx 0.8$ ppm, values at different pHs coincide. The insert shows the CH–$CH(CH_3)_2$ fragment of the Val or Leu side chains. (II) Average line width, $(LW_A + LW_B)/2$, for each geminal CH_3 pair of the six Val or Leu plotted against the average chemical shift of the same pair, $(\delta_A + \delta_B)/2$, at pH 4.8 (●) and 12.0 (○). The insert shows the $CH(CH_3)_2$ fragment of the Val and Leu side chains. The curves result from arbitrary interpolations between points.

and 75 °C, while 23 at the same residue is fairly temperature independent. In the same temperature range we observe the transition from slow to rapid flip motion of the Tyr-31 ring responsible for the high field shift of methyls 23 and 25 (De Marco et al., 1979). Thus, it can be inferred that the valine side chain is oriented so that methyl 23 is unaffected by the dynamics of the aromatic side chain, while the geminal methyl 25 shows a progressive downfield shift with increasing temperature. The only other methyl group which exhibits a rather strong temperature dependence among those shown in Figure 6 is the one marked 1, i.e., the γ-CH_3 from Thr-1, which is shifted upfield by ca. 0.09 ppm between 25 and 75 °C. This can be attributed to H bonding or a salt bridge interaction between Thr-1 and some neighboring group or even to an interaction between the side chain and the free terminal amino group. The mobility of an N-terminal L-Thr side chain in unprotected linear peptides is known to be fairly restricted (Ptak et al., 1978).

As a general trend, shifted methyl resonances move toward random-coil positions by increasing either pH or temperature. The temperature-dependence diagram shown in Figure 6 reveals that some methyl resonances, such as 1 and 14, exhibit the parabolic trend observed for 24 and 25 (De Marco et al., 1979), while other show inflections (3, 10, 11, 12, and 18) or discontinuities (19, 21, and 22) between 40 and 50 °C, which could be related to the slow to rapid motion transition of Tyr-31 (De Marco et al., 1979). At all events, the chemical shift variations between 25 and 75 °C correspond only to a small fraction of the overall conformational contribution to the chemical shifts, which is consistent with small influence of ring flips to the resonance positions of the aliphatic protons (Perkins & Wüthrich, 1979).

As noticed from Table II, the more each couple of valyl or leucyl methyls is displaced from the random-coil position, the larger the chemical shift difference becomes between geminal CH_3 resonances. Figure 8I shows a plot of the relative parameter $(\delta_A - \delta_B)$ for the geminal methyls (A and B) of the four valines and the two leucines in PSTI vs. the average chemical shift of each pair $(\delta_A + \delta_B)/2$ at pH 4.8 and 12. At both pHs, $\delta_A - \delta_B$ shows a minimum at about the random-coil value of $(\delta_A + \delta_B)/2$ (ca. 0.95 ppm). Table II also reveals a chemical shift dependence of methyl resonance line width. The average line width of each pair of valine or leucine methyls $(LW_A + LW_B)/2$ is plotted vs. $(\delta_A + \delta_B)/2$ in Figure 8II. As observed for the relative chemical shift, the line width of methyl resonances goes through a minimum when CH_3 groups resonate near the random-coil position. In both plots (Figure 8) the leucine pairs 17–18 and 19–22 yield the most consistent representation of data, favoring the assignment proposed above.

A reduced mobility about the C^α–C^β bond for valyl and C_β–C_γ for leucyl residues (Figure 8I, insert) manifests in a large chemical shift difference for resonances from geminal methyl groups. On the other side, the methyls strongly influenced by neighbor side chains—such as those buried in the hydrophobic pockets surrounding aromatic rings—yield increased signal line widths, which can be ascribed to a hindered rotation about the CH–CH_3 bond (Figure 8II, insert). Thus, both the conformation-dependent methyl chemical shifts and line widths may afford useful ^1H NMR probes that monitor strain effects reflecting different microenvironments in proteins.

References

Bartelt, D. C., & Greene, L. J. (1971) *J. Biol. Chem. 246*, 2218–2229.

Bothner-By, A. A. (1970) *Adv. Magn. Reson. 4*, 195–316.

Brown, L. R., De Marco, A., Wagner, G., & Wüthrich, K. (1976) *Eur. J. Biochem. 62*, 103–107.

Bundi, A., & Wüthrich, K. (1979) *Biopolymers 18*, 285–297.

Campbell, I. D., Dobson, C. M., Williams, R. J. P., & Xavier, A. V. (1973) *J. Magn. Reson. 11*, 172–181.

Campbell, I. D., Dobson, C. M., & Williams, R. J. P. (1975a) *Proc. R. Soc. London, Ser. A 345*, 23–40.

Campbell, I. D., Dobson, C. M., & Williams, R. J. P. (1975b) *Proc. R. Soc. London, Ser. A 345*, 41–59.

Cramer, J. A., Marchesi, V. T., & Armitage, I. M. (1980) *Biochim. Biophys. Acta 595*, 235–243.

Deisenhofer, J., & Steigemann, W. (1975) *Acta Crystallogr., Sect. B B31*, 238–250.

De Marco, A. (1977) *J. Magn. Reson. 26*, 527–528.

De Marco, A., & Wüthrich, K. (1976) *J. Magn. Reson. 24*, 201–204.

De Marco, A., Menegatti, E., & Guarneri, M. (1979) *Eur. J. Biochem. 102*, 185–194.

Greene, L. J., & Bartelt, D. C. (1969) *J. Biol. Chem. 244*, 2646–2657.

Greene, L. J., Pubols, M. H., & Bartelt, D. C. (1976) *Methods Enzymol. 45*, 813–825.

Katz, J., Troll, W., Adler, S. W., & Levitz, M. (1977) *Proc. Natl. Acad. Sci. U.S.A. 74*, 3754–3757.

Lauterwein, J., Lazdunski, M., & Wüthrich, K. (1978) *Eur. J. Biochem. 92*, 361–371.

Markley, J. L. (1975) *Acc. Chem. Res. 8*, 70–80.

Meyn, M. S., Rossman, T., & Troll, W. (1977) *Proc. Natl. Acad. Sci. U.S.A. 74*, 1152–1156.

Navon, G., & Polak, M. (1974) *Chem. Phys. Lett. 25*, 239–242.

Perkins, S. J., & Wüthrich, K. (1979) *Biochim. Biophys. Acta 576*, 409–423.
Ptak, M., Heitz, A., & Dreux, M. (1978) *Biopolymers 17*, 1129–1148.
Schmidth-Aderjan, U., Rösch, P., Frank, R., & Hengstenberg, W. (1979) *Eur. J. Biochem. 96*, 43–48.
Sternlicht, H., & Wilson, D. (1967) *Biochemistry 6*, 2881–2892.
Troll, W., Klassen, A., & Janoff, A. (1970) *Science (Washington, D.C.) 169*, 1211–1213.
Tschesche, H. (1967) *Hoppe-Seyler's Z. Physiol. Chem. 348*, 1653–1659.
Tschesche, H., & Wachter, E. (1970) *Eur. J. Biochem. 16*, 187–198.
Wagner, G., & Wüthrich, K. (1979) *J. Mol. Biol. 134*, 75–94.
Witkin, E. M. (1976) *Bacteriol. Rev. 40*, 869–907.
Wüthrich, K., & Wagner, G. (1978) *Trends Biochem. Sci. (Pers. Ed.) 3*, 227–230.

Hydrodynamic Properties of Bovine Cardiac Troponin C†

David M. Byers and Cyril M. Kay*

ABSTRACT: The size and shape of bovine cardiac troponin C (TN-C) in solution have been examined by gel filtration, ultracentrifugation, and viscosity in the presence and absence of Ca^{2+}. Cardiac TN-C ($-Ca^{2+}$) has an intrinsic sedimentation coefficient, $s^0_{20,w}$, of 1.87 S and a Stokes radius, R_S, of 26.3 Å as determined by gel chromatography on Sephacryl S-300. In 2 mM Ca^{2+}, $s^0_{20,w}$ is increased to 2.04 S and R_S is decreased to 24.3 Å, indicating a conformational change to a more compact structure. Furthermore, the intrinsic viscosity of TN-C in the absence of Ca^{2+} (6.4 mL/g) is reduced to 5.4 mL/g when Ca^{2+} is added. Sedimentation equilibrium studies indicate that the effects of Ca^{2+} are not due to changes in the molecular weight of the protein. The hydrodynamic data suggest that TN-C is a moderately asymmetric protein with an axial ratio of 4–6.

The Ca^{2+} regulation of striated muscle occurs at the level of the thin filament via the troponin–tropomyosin complex [for recent reviews, see Adelstein & Eisenberg (1980); McCubbin & Kay (1980)]. Troponin consists of three nonidentical subunits: TN-C (the Ca^{2+}-binding subunit), TN-I (the inhibitory subunit), and TN-T (the tropomyosin-binding subunit). The signal for muscle contraction apparently involves the binding of Ca^{2+} to TN-C although subsequent events, which ultimately lead to activation of the actomyosin adenosinetriphosphatase, are not understood in molecular detail. It is clear that any refined model of thin filament regulation must include some structural knowledge of the regulatory proteins involved. This knowledge can be obtained either from X-ray analysis or from optical and hydrodynamic studies in solution.

Most of the current information about the structure and function of troponin has been obtained with the proteins from rabbit skeletal muscle. However, troponin subunits from cardiac muscle appear to be qualitatively similar to their skeletal counterparts, with minor differences being attributable to the particular requirements of cardiac muscle regulation (McCubbin & Kay, 1980). The most extensively studied cardiac subunit, bovine cardiac TN-C, has been sequenced (van Eerd & Takahashi, 1975) and has a molecular weight of 18 459. This TN-C contains two cysteine and three tyrosine residues but no tryptophan or histidine. Like rabbit skeletal TN-C, this protein has two high-affinity ($K_a \sim 10^7$ M^{-1}) Ca^{2+}-binding sites, which can also bind Mg^{2+} (Hincke et al., 1978; Holroyde et al., 1980). Cardiac TN-C differs, however, in that it contains only one Ca^{2+}-specific site ($K_a \sim 2 \times 10^5$ M^{-1}) (Leavis & Kraft, 1978; Holroyde et al., 1980). So far, no X-ray structural determination has been reported for TN-C from any source, although crystals suitable for this purpose have recently been obtained for chicken skeletal TN-C (Strasburg et al., 1980). In this paper, the structural properties of bovine cardiac TN-C in solution are investigated by hydrodynamic methods. The results indicate that TN-C is a moderately asymmetric molecule that undergoes a conformational change when Ca^{2+} is present.

Experimental Procedures

Protein Preparation. Bovine cardiac TN-C was initially isolated from crude troponin (Tsukui & Ebashi, 1973) by chromatography on DEAE-Sephadex[1] in 6 M urea as previously described (Burtnick et al., 1975). Pooled fractions containing TN-C were dialyzed against 50 mM Tris-HCl, 2 mM EGTA, and 0.5 mM DTT (pH 7.5) and applied to a DEAE-Sephadex A25 column (2 × 20 cm) equilibrated with the same buffer. TN-C was eluted with a linear 0–0.8 M NaCl gradient at 4 °C. The dominant peak eluting at ~0.4 M NaCl was pure TN-C, as judged by $NaDodSO_4$–polyacrylamide gel electrophoresis (Weber & Osborn, 1969).

Analytical solutions were prepared by dissolving lyophilized TN-C in 0.2 M KMED buffer (0.2 M KCl, 50 mM Mops, 1 mM EGTA, and 1 mM DTT) at pH 7.2, followed by dialysis against this buffer for at least 20 h (48 h for densitometry or sedimentation equilibrium studies). Buffers representing the

† From the Medical Research Council Group in Protein Structure and Function, Department of Biochemistry, University of Alberta, Edmonton, Alberta, T6G 2H7 Canada. *Received May 14, 1981.* This work was supported by the Medical Research Council of Canada and the Alberta Heritage Trust Fund. D.M.B. is the recipient of a postgraduate studentship from the Medical Research Council of Canada.

[1] Abbreviations: EGTA, ethylene glycol bis(β-aminoethyl ether)-*N,N,N',N'*-tetraacetic acid; BSA, bovine serum albumin; Mops, 3-(*N*-morpholino)propanesulfonic acid; DTT, dithiothreitol; 0.2 M KMED buffer, 0.2 M KCl, 50 mM Mops, 1 mM EGTA, and 1 mM DTT; DEAE, diethylaminoethyl; Tris, tris(hydroxymethyl)aminomethane; $NaDodSO_4$, sodium dodecyl sulfate; NMR, nuclear magnetic resonance.

0006-2960/82/0421-0229$01.25/0